



Evolution of crack paths and compliance in round bars under cyclic tension and bending

J. Toribio, J.C. Matos, B. González, J. Escudra
University of Salamanca, Spain
toribio@usal.es

ABSTRACT. The aim of this paper is to calculate how the surface crack front and the dimensionless compliance evolve in cracked cylindrical bars subjected to cyclic tension or bending with different initial crack geometries (crack depths and aspect ratios). To this end, a computer application (in the Java programming language) that calculates the crack front's geometric evolution and the dimensionless compliance was made by discretizing the crack front (characterized with elliptical shape) and assuming that every point advances perpendicularly to the crack front according to the Paris law, and using a three-parameter stress intensity factor (SIF). The results show that in fatigue crack propagation, relative crack depth influences more on dimensionless compliance than the aspect ratio, because the crack front tends to converge when the crack propagates from different initial geometries, showing greater values for tension than for bending. Furthermore, during fatigue crack growth, materials with higher values of the exponent of the Paris law produce slightly greater dimensionless compliance and a better convergence between the results for straight-fronted and circular initial cracks.

KEYWORDS. Cracked round bar; Numerical modelling; Paris law; Fatigue crack growth; Dimensionless compliance.

INTRODUCTION

The problem of fatigue crack propagation in round bars is of great interest in fracture mechanics, applied to linear structural elements. These components, usually subjected to oscillating load, may fracture after surface fatigue crack growth, frequently with semi-elliptical flaws contained in a plane perpendicular to the loading axis. Several criteria have been stated in the past to characterize fatigue crack growth in these geometries, e.g., prediction of the 90° intersecting angle of the crack with the surface or the iso- K criterion along the crack front [1]. The most used are those based on the Paris-Erdogan law [2-6], requiring the knowledge of the dimensionless stress intensity factor (SIF), Y , along the crack front in the round cracked bar. It has been deduced by several authors following different procedures: compliance methods, finite element analysis, boundary integral equation methods, experimental techniques, etc. [1, 7-10]. Dimensionless compliance in round cracked bars under tension or bending depends on the crack geometry. If the crack is characterized by an elliptical shape, there are two factors exerting influence: the relative crack depth (crack depth divided by the diameter), which causes an increase of its value, and the aspect ratio (ratio between the crack depth and the other semiaxis of the ellipse), which causes a decrease of its value [3, 11]. Thus, there is a relation between the change in compliance during fatigue crack growth and the crack geometry evolution, depending on the specimen material, the initial crack geometry and the type of applied load [10, 12].

NUMERICAL MODELLING

A computer program in the Java programming language was developed to determine the geometrical evolution of the crack front according to the Paris law, for a transverse surface crack in a cylindrical geometry subjected to cyclic tension loading or cyclic bending moment (Fig. 1). This would be the basis to determine the change taking place in the dimensionless compliance of the round bar during the fatigue crack propagation process.

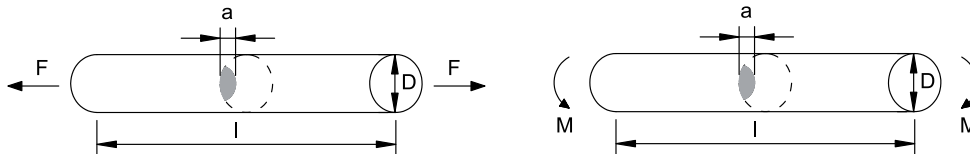


Figure 1: Cracked bar under tension loading (left) and bending moment (right).

Aspect ratio

The basic hypothesis of the modelling consisted of assuming that the crack front can be modelled as an ellipse with centre on the bar surface [12] and the fatigue propagation takes place in a direction perpendicular to this crack front, following a Paris-Erdogan law [13],

$$\frac{da}{dN} = C \Delta K^m \quad (1)$$

Every elliptical arc of the crack front was divided in z segments with exactly the same length using the Simpson's rule in order to discretize the front. The point on the round bar surface was not taken into account, since it presents some difficulties regarding the computation of the dimensionless SIF (there is a plane stress state on the crack surface). After that, every single point was shifted according to the Paris-Erdogan law perpendicular to the front and so as to keep constant the maximum crack depth increment, $\Delta a(\max) \equiv \max \Delta a_i$, all over the process [6]. The advance of every front point, Δa_i , can be obtained from the maximum crack increment and the ratio of the dimensionless SIFs,

$$\Delta a_i = \Delta a(\max) \left[\frac{Y_i}{Y(\max)} \right]^m \quad (2)$$

The newly obtained points, fitted by the least squares method, generate a new ellipse with which the process is repeated iteratively until the desired crack depth is reached. Due to the existing symmetry, only half of the problem was used for the computations.

Dimensionless SIF

The dimensionless SIF, Y , depends on three-parameters for the crack modelled as an ellipse with centre on the round bar surface and its value depends on the crack geometry (depth and aspect ratio) and on the point on the front where it is calculated. The dimensionless SIF used in the computations is that proposed by Shin and Cai [10] obtained by the finite element method and the virtual crack extension technique, whose value is function of the relative crack depth a/D , the crack aspect ratio a/b , and the position of the point considered on its front x/b (Fig. 2).

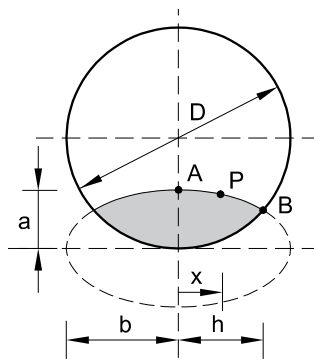


Figure 2: Elliptical crack model used by Shin and Cai.



The fitting of the results provides a three-parametrical expression which is defined as a function of the coefficients M_{ijk} for tension with free sample ends [10], i.e., unrestrained bending during tension,

$$Y = \sum_{i=0}^2 \sum_{j=0}^7 \sum_{k=0}^2 M_{ijk} \left(\frac{a}{b}\right)^i \left(\frac{a}{D}\right)^j \left(\frac{x}{b}\right)^k \quad (3)$$

and the coefficients N_{ijk} for bending [10],

$$Y = \sum_{i=0}^2 \sum_{j=0}^6 \sum_{k=0}^2 N_{ijk} \left(\frac{a}{b}\right)^i \left(\frac{a}{D}\right)^j \left(\frac{x}{b}\right)^k \quad (4)$$

Dimensionless compliance

Experimentally the geometrical evolution of the crack front in a cylindrical bar can be observed *post mortem* (once fractured) and there are several techniques to mark the front according to the material studied. It is possible to relate the crack front geometry with compliance, one of the few characteristics which can be measured during the crack propagation [14].

If tensile load is applied, it is obtained that the local displacement u is related to the applied force F through compliance λ as follows:

$$u = \lambda F \quad (5)$$

If bending is applied, in this case the angle φ is related to the applied moment M through compliance λ as follows:

$$\varphi = \lambda M \quad (6)$$

The strain energy U can be expressed taking into account the equivalence between the energy release rate G and the SIF in plane strain K ,

$$dU = GdA = \frac{K^2(1-\nu^2)}{E} dA \quad (7)$$

where ν is the Poisson coefficient and dA the differential of the cracked area.

On the other hand, the strain energy for a cracked bar subjected to tensile load is, introducing the value $d\mu$ from Eq. (5),

$$dU = \frac{1}{2} F d\mu = \frac{1}{2} F^2 d\lambda \quad (8)$$

and the strain energy for a cracked bar subjected to bending is, introducing the value $d\mu$ from the Eq. (6),

$$dU = \frac{1}{2} M d\varphi = \frac{1}{2} M^2 d\lambda \quad (9)$$

The SIF in plane strain for the geometry of the study can be obtained as follows:

$$K = Y\sigma\sqrt{\pi a} \quad (10)$$

where the stress σ for axial tension is calculated as:

$$\sigma = \frac{4F}{\pi D^2} \quad (11)$$

and the maximum stress σ for bending is calculated as:

$$\sigma = \frac{32M}{\pi D^3} \quad (12)$$

If equations for strain energy are made equal and introducing values K and σ , the isolated compliance is obtained for tension loading:

$$\lambda = \frac{32(1-\nu^2)}{\pi D^4 E} \int_0^a Y^2 a dA \quad (13)$$

and for bending moment,



$$\lambda = \frac{2048(1-\nu^2)}{\pi D^6 E} \int_0^a Y^2 a dA \quad (14)$$

Solving the integral which appears in Eq. (13) and (14) is not trivial. In order to achieve that, the Cartesian coordinates (x, y) were change into parametrical coordinates (a, θ) , relating themselves through the expressions:

$$x = b \cos \theta \quad (15)$$

$$y = a \sin \theta \quad (16)$$

where the correspondence between angles δ and θ , deducted from Fig. 3, is as follows,

$$\tan \delta = \frac{y}{x} = \frac{a}{b} \tan \theta \quad (17)$$

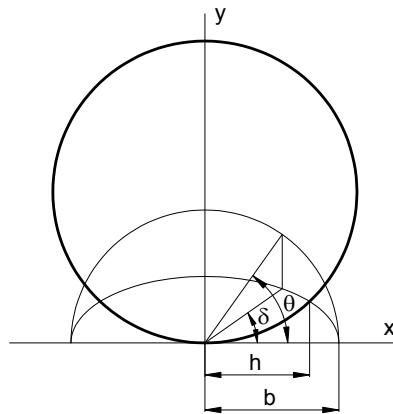


Figure 3: Relationship between δ and θ angles.

The differential of the ellipse area modelling the crack advance is:

$$dA = dx \wedge dy \quad (18)$$

differentiating the coordinates (x, y) according to the new coordinates (a, θ) ,

$$dx = b'(a) \cos \theta da - b \sin \theta d\theta \quad (19)$$

$$dy = \sin \theta da + a \cos \theta d\theta \quad (20)$$

and substituting these expressions on the Eq. (18), it is obtained:

$$dA = (ab'(a) \cos^2 \theta + b \sin^2 \theta) da \wedge d\theta \quad (21)$$

The problem that arises in calculating Eq. (21) can be found in the previous knowledge of the variation of the parameter b with the crack depth a . The definition of the derivative at a point can be used to this purpose,

$$b'(a) \approx \frac{b(a + \Delta a) - b(a)}{\Delta a} \quad (22)$$

Introducing Eq. (21) in Eq. (13), that allows the computation of the compliance in a cracked round bar subjected to axial tensile loading, it is obtained:

$$\lambda = \frac{64(1-\nu^2)}{\pi D^4 E} \int_0^a \int_{a \cos \frac{\theta}{b}}^{\pi/2} Y^2 a (ab'(a) \cos^2 \theta + b \sin^2 \theta) d\theta da \quad (23)$$

Introducing Eq. (21) in Eq. (14), which allows calculating compliance in a cracked round bar subjected to bending loading, it is obtained:

$$\lambda = \frac{4096(1-\nu^2)}{\pi D^3 E} \int_0^a \int_{a \cos \frac{b}{b}}^{\pi/2} Y^2 a (ab'(a) \cos^2 \theta + b \sin^2 \theta) d\theta da \quad (24)$$

where f is defined as the dimensionless compliance due to tensile or bending load:

$$f = \int_0^a \int_{a \cos \frac{b}{b}}^{\pi/2} Y^2 \frac{a}{D^3} (ab'(a) \cos^2 \theta + b \sin^2 \theta) d\theta da \quad (25)$$

The dimensionless compliance value can be calculated incrementally with the crack growth, where the integral,

$$f = \sum_i \int_{a_i}^{a_{i+1}} \int_{a \cos \frac{b}{b}}^{\pi/2} R d\theta da \quad (26)$$

it is solved using the trapezoidal rule (where R is the corresponding expression according to Eq. (25)), following the scheme on Fig. 4, dividing every crack increment in eight parts for half of the problem, so they correspond with the coordinate's isolines (a, θ).

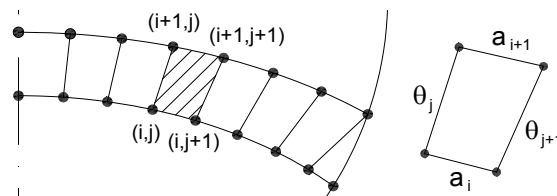


Figure 4: Divisions with the isolines used in the trapezoidal rule.

The compliance increment in every crack advance is calculated using the following expression,

$$f = \sum_i (a_{i+1} - a_i) \left(\sum_{j=0}^7 (\theta_{j+1} - \theta_j) \frac{(R(i,j) + R(i,j+1) + R(i+1,j) + R(i+1,j+1))}{4} + \frac{(\theta_8 - \theta_7) (R(i,7) + R(i+1,7) + R(i,8))}{2 \cdot 3} \right) \quad (27)$$

In order to obtain the dimensionless compliance of the initial crack, the process is similar to that just described, but easier, because it considers that every previous crack front has the same aspect ratio as the initial one.

NUMERICAL RESULTS AND DISCUSSION

Fatigue cracking paths

The study of the convergence was performed to obtain the number of segments in which each ellipse is divided, $\xi=14$, and the value of the maximum crack increase, $\Delta a(\max)=D/1000$. The geometrical evolution of the crack front, characterized as part of the ellipse, was determined for every relative crack depth, a/D , through the aspect ratio, a/b , for materials with Paris exponent $m=2, 3$ and 4 , starting from different initial crack geometries (corresponding to the beginning of each curve) under cyclic tension loading and cyclic bending moment (Figs. 5 to 7). Under fatigue loading, different initial crack configurations tend to a preferential path (in a plot a/b - a/D), the convergence being faster for higher values of the m coefficient of the Paris law and greater for the bending loading than for the tensile loading. When subjected to bending, growth curves generally present lower values for the a/b parameter than under tension, with the exception of the deepest cracks growing from an initial crack aspect ratio $(a/b)_0 \approx 0$. If the initial crack is circular, the aspect ratio a/b diminishes with the crack growth, whereas when the initial crack is quasi-straight, the aspect ratio a/b increases at the beginning and decreases later (with the exception of initially deep cracks with $(a/D)_0 \approx 0.5$, where the aspect ratio a/b always increases), cf. Figs. 5 to 7.

It is observed that results depend on the exponent of the Paris law, so that for $m=2$ and $m=3$ the crack fronts are more distant between them than for $m=3$ and $m=4$, where the $m=3$ front is between $m=2$ and $m=4$. In the case of growth from *circular initial cracks*, the maximum discrepancy with regard to the crack fronts appears for intermediate cracks ($a/D \sim 0.5$), a/b being lower for higher values of m -exponent in the Paris law. In the case of growth from *quasi-straight initial cracks*, the maximum discrepancy in



the matter of the crack fronts appears for short ($(a/b)_0 \sim 0.3$) and long ($(a/b)_0 \sim 0.7$) cracks, whereas for intermediate ($(a/b)_0 \sim 0.5$) cracks the results for different Paris coefficient m almost match. For short cracks a/b is higher for greater m , whereas for long cracks a/b is higher for lower values of m (again with the exception of initially deep cracks with $(a/D)_0 \approx 0.5$).

Dimensionless compliance

The evolution of the dimensionless compliance f during fatigue crack propagation is shown in Figs. 8 to 10, for different initial crack depths, initial crack aspect ratios (quasi-straight front and circular front), and different loading conditions (tension and bending). In cracked cylindrical bars, dimensionless compliance f depends on the loading conditions, on the relative crack depth a/D and on the crack aspect ratio a/b . During fatigue crack growth starting from different initial crack geometries, it is observed how the dimensionless compliance f increases with the relative crack depth a/D and how the influence of the crack aspect ratio a/b is lower as the crack grows, due to the marked geometrical convergence taking place for the deepest cracks, in which the compliance reaches the highest values. The dimensionless compliance f for initially quasi-straight cracks is approximately twice than that for initially circular crack, both being really small at the beginning (initial cracks) and increasing clearly and approaching between them under fatigue. The dimensionless compliance f in the cracked bars is higher under tensile loading than under bending moment, the ratio being as high as five for the deepest cracks of the present analysis ($a/D=0.7$). The f - a/D plots starting from an initially circular crack front and from an initially quasi-straight crack front are closer when (i) the applied load is bending instead of tension, (ii) the exponent m of the Paris law is higher, (iii) the initial crack depth $(a/D)_0$ is lower. Furthermore, during fatigue crack growth, materials with higher values of the Paris parameter m produce slightly greater dimensionless compliance.

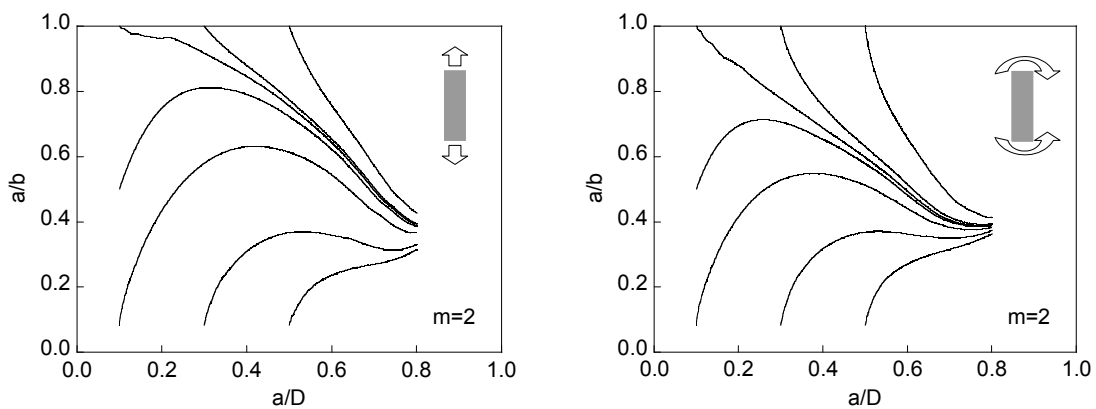


Figure 5: Evolution of the aspect ratio a/b with crack growth (represented by the relative crack depth a/D) for $m=2$, starting from different initial crack geometries under tension loading (left) and bending moment (right).

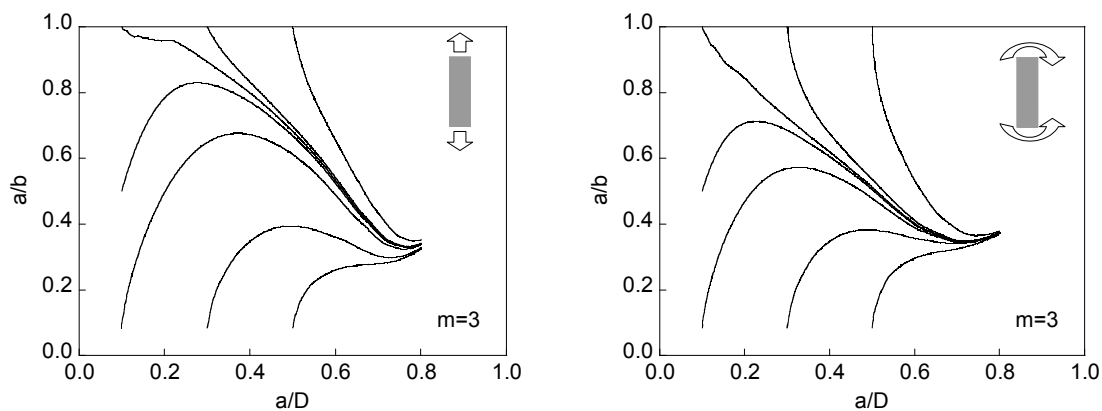


Figure 6: Evolution of the aspect ratio a/b with crack growth (represented by the relative crack depth a/D) for $m=3$, starting from different initial crack geometries under tension loading (left) and bending moment (right).

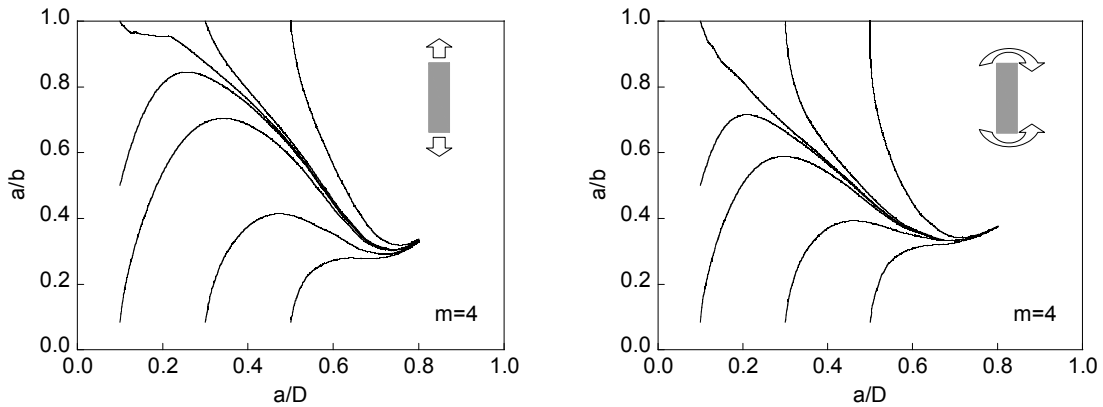


Figure 7: Evolution of the aspect ratio a/b with crack growth (represented by the relative crack depth a/D) for $m=4$, starting from different initial crack geometries under tension loading (left) and bending moment (right).

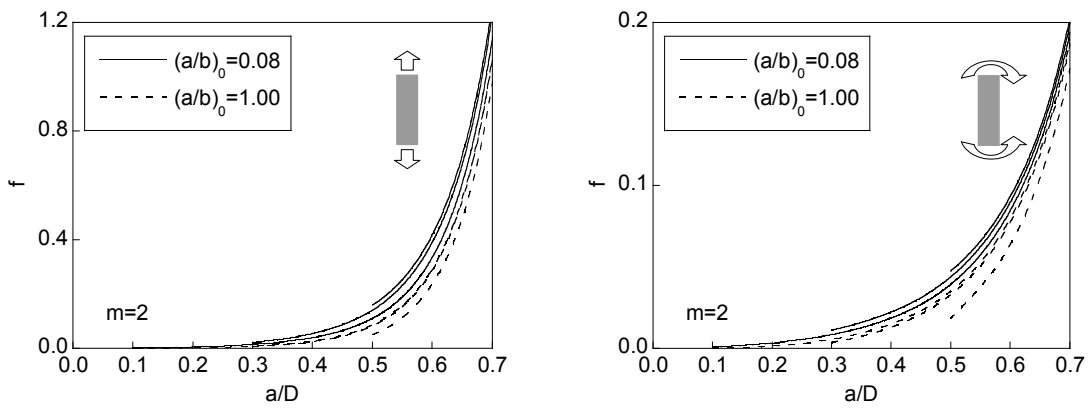


Figure 8: Evolution of the dimensionless compliance f with crack growth (represented by the relative crack depth a/D) for $m=2$, starting from different initial crack geometries under tension loading (left) and bending moment (right).

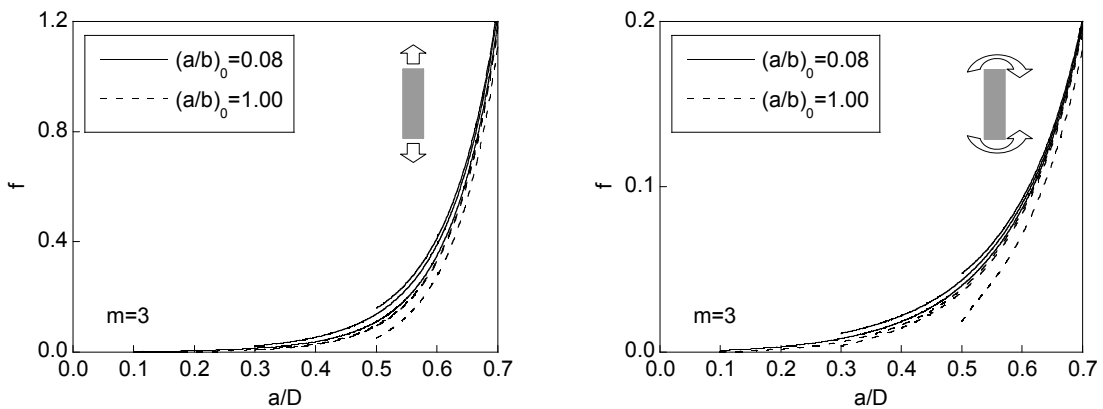


Figure 9: Evolution of the dimensionless compliance f with crack growth (represented by the relative crack depth a/D) for $m=3$, starting from different initial crack geometries under tension loading (left) and bending moment (right).

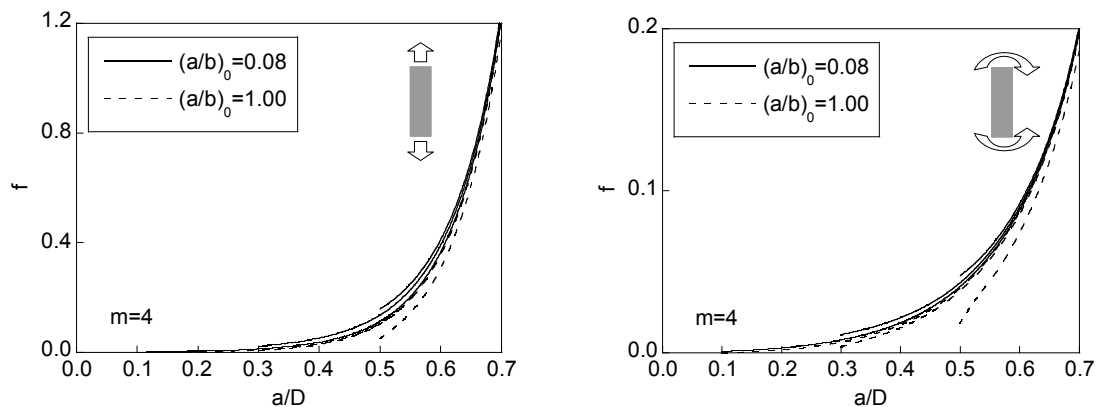


Figure 10: Evolution of the dimensionless compliance f with crack growth (represented by the relative crack depth a/D) for $m=4$, starting from different initial crack geometries under tension loading (left) and bending moment (right).

CONCLUSIONS

The following conclusions have been drawn from this work regarding the evolution of crack paths and compliance in round bars under cyclic tension or cyclic bending:

- According to the Paris-Erdogan law, in fatigue propagation the different initial crack geometries tend to a unique path on the a/b vs. a/D plot, this convergence being faster for higher coefficients m of Paris and quicker for bending than for tension loading.
- With quasi-circular initial geometries, the crack aspect ratio a/b diminishes with the crack growth, whereas when the initial crack is quasi-straight, the aspect ratio increases at the beginning and decreases at the end (with the exception of initially deep crack).
- In fatigue crack propagation, relative crack depth a/D influences more on dimensionless compliance f than the aspect ratio a/b , because the crack fronts tend to converge as the cracks propagate from different initial geometries.
- The f - a/D plots starting from an initially circular crack front and from an initially quasi-straight crack front are closer when the applied load is bending, the exponent m of the Paris law is higher or the initial crack depth $(a/D)_0$ is lower.

ACKNOWLEDGEMENTS

The authors wish to acknowledge the financial support provided by the following Spanish Institutions: MICYT (Grant MAT2002-01831), MEC (Grant BIA2005-08965), MICINN (Grants BIA2008-06810 and BIA2011-27870) and JCyL (Grants SA067A05, SA111A07 and SA039A08).

REFERENCES

- [1] Carpinteri, A., Shape change of surface cracks in round bars under cyclic axial loading, *Int. J. Fatigue*, 15 (1993) 21-26.
- [2] Shih, Y.-S., Chen, J.-J., Analysis of fatigue crack growth on a cracked shaft, *Int. J. Fract.*, 19 (1997) 477-485.
- [3] Couroneau, N., Royer, J., Simplified model for the fatigue growth analysis of surface cracks in round bars under mode I, *Int. J. Fatigue*, 20 (1998) 711-718.
- [4] Lin, X.B., Smith, R.A., Shape growth simulation of surface cracks in tension fatigued round bars, *Int. J. Fatigue*, 19 (1997) 461-469.
- [5] Shin, C.S., Cai, C.Q., Evaluating fatigue crack propagation properties using a cylindrical rod specimen, *Int. J. Fatigue*, 29 (2007) 397-405.
- [6] Toribio, J., Matos, J.C., González, B., Escudra, J., Numerical modelling of crack shape evolution for surface flaws in round bars under tensile loading, *Eng. Fail. Anal.*, 16 (2009) 618-630.
- [7] Astiz, M.A., An incompatible singular elastic element for two- and three-dimensional crack problems, *Int. J. Fract.*, 31 (1986) 105-124.
- [8] Carpinteri, A., Elliptical-arc surface cracks in round bars, *Fatigue Fract. Eng. Mater. Struct.*, 15 (1992) 1141-1153.



- [9] Levan, A., Royer, J., Part-circular surface cracks in round bars under tension, bending and twisting, *Int. J. Fract.*, 61 (1993) 71-99.
- [10] Shin, C.S., Cai, C.Q., Experimental and finite element analyses on stress intensity factors of elliptical surface crack in a circular shaft under tension and bending, *Int. J. Fract.*, 129 (2004) 239-264.
- [11] Rubio, L., Muñoz-Abella, B., Loaiza, G., Static behaviour of a shaft with an elliptical crack, *Mech. Syst. Signal Process.*, 25 (2011) 1674-1686.
- [12] Toribio, J., Matos, J.C., González, B., Escudra, J., Compliance evolution in round cracked bars under tensile fatigue, *Eng. Fract. Mech.*, 78 (2011) 3243-3252.
- [13] Paris, P.C., Erdogan, F., A critical analysis of crack propagation laws, *J. Basic Eng.*, 85D (1963) 528-534.
- [14] Cai, C.Q., Shin, C.S., A normalized area-compliance method for monitoring surface crack development in a cylindrical rod, *Int. J. Fatigue*, 27 (2005) 801-809.